Hyperspectral analysis of lithologies in the Arctic in areas with abundant lichen cover

Sara Salehi

Lithological mapping using remote sensing depends, in part, on the identification of rock types by their spectral characteristics. Chemical and physical properties of minerals and rocks determine their diagnostic spectral features throughout the electromagnetic spectrum. Shifts in the position and changes in the shape and depth of these features can be explained by variations in chemical composition of minerals. Detection of such variations is vital for discriminating minerals with similar chemical composition. Compared with multispectral image data, airborne or spaceborne hyperspectral imagery offers higher spectral resolution, which makes it possible to estimate the mineral composition of the rocks under study without direct contact.

Arctic environments provide challenging ground for geological mapping and mineral exploration. Inaccessibility commonly complicates ground surveys, and the presence of ice, vegetation and rock-encrusting lichens hinders remote sensing surveys. This study addresses the following objectives:

1. Modelling the impact of lichen on the spectra of the rock substrate;
2. Identification of a robust lichen index for the deconvolution of lichen and rock mixtures and
3. Multiscale hyperspectral analysis of lithologies in areas with abundant lichens.

Modelling the impact of lichen cover

Spectral mixing of lichens and bare rock can shift the wavelength positions of characteristic absorption features and complicate the spectral mapping of minerals and lithologies. Salehi *et al.* (2017) investigated how surficial lichen cover affects the characteristics of shortwave infrared mineral absorption features and the efficiency of automated extraction of absorption features. For this purpose, mixed spectra were synthetically generated from laboratory spectra of common rock-forming minerals and lichens. Wavelength displacements of characteristic absorption features for each mixed spectrum were then analysed as a function of lichen cover percentage (see an example in Fig. 1). By quantifying lichen
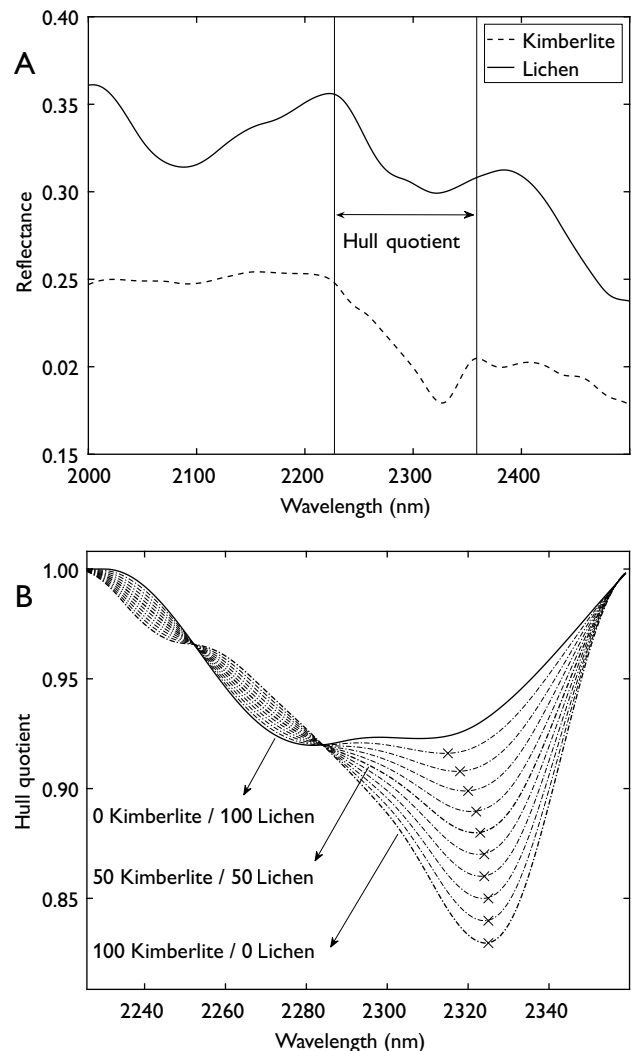

Fig. 1. **A**: Averaged spectra of pure rock and lichen for a kimberlite substrate in shortwave infrared range. **B**: The corresponding hull quotient (Clark & Roush 1984) and band centres of mixed spectra associated with the antigorite absorption feature. The 10% spectral intervals used to investigate the main absorption features are highlighted. **x**: wavelength positions of local minima (Salehi *et al.* 2017).

cover effects on mineral absorption features, this study highlights the importance cautious interpretation in areas characterised by abundant, lichen-covered outcrops. This can be of significant importance for mineral and deposit identification, because slightly shifted features for a given spectrum caused by lichen cover can be erroneously identified as a path to a deposit. Salehi *et al.* (2017) showed that spectral shifts caused by lichens are not constant, i.e. each mineral spectral feature may be affected differently depending on the shape of the lichen spectrum. For example, the absorption feature related to the chlorite mineral group around 2254 nm is shifted towards longer wavelength, while the one around 2320 nm is shifted towards shorter wavelength and the 2380 nm band maintains its spectral characteristics. Spectral shifts are not only related to rock/lichen proportions but also to the modal abundance of minerals in certain rock types. Background minerals and associated overlapping features will have an effect on the related absorption depth and play a critical role in the scale of wavelength displacement.

Identification of a robust lichen index

The ability to distinguish a lichen cover from its rock/mineral substrate is important, and decomposition of a mixed pixel into a collection of pure reflectance spectra can improve the use of hyperspectral methods for mineral exploration. In order to identify spectral indices that can directly reflect the ratio of the rock and lichen in hyperspectral data, a number of index structures were assigned to an optimisation algorithm, which was tasked to find the best values for the location of the bands along the reflectance spectra measured in the laboratory (Salehi *et al.* 2016). In order to further investigate the functionality of the indices for the airborne platform, the spectra were resampled to HyMAP resolution.

The indices proposed by Salehi *et al.* (2016) proved robust to the type of the substrate rock and permitted an estimate of the lichen cover with acceptable, albeit varying, levels of error. The results revealed that the ratio between $R_{894-1246}$ and R_{1110} explains most of the variability in the hyperspectral data at the original laboratory resolution ($R^2=0.769$). However, the normalised index incorporating $R_{1106-1121}$ and $R_{904-1251}$ yields the best results for the HyMAP resolution ($R^2=0.765$).
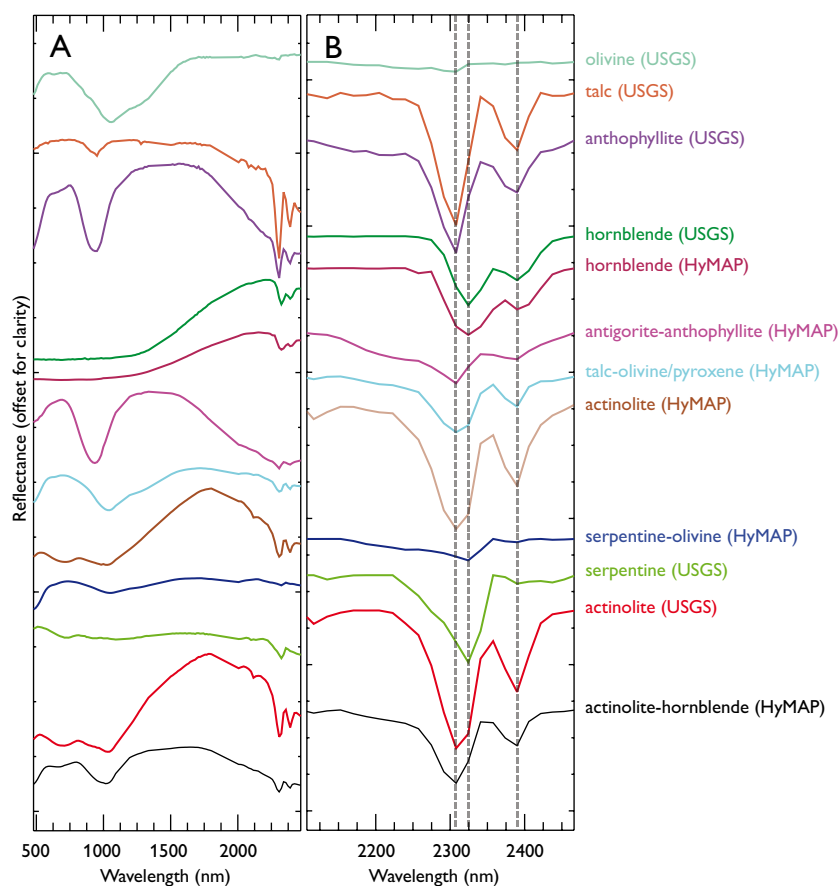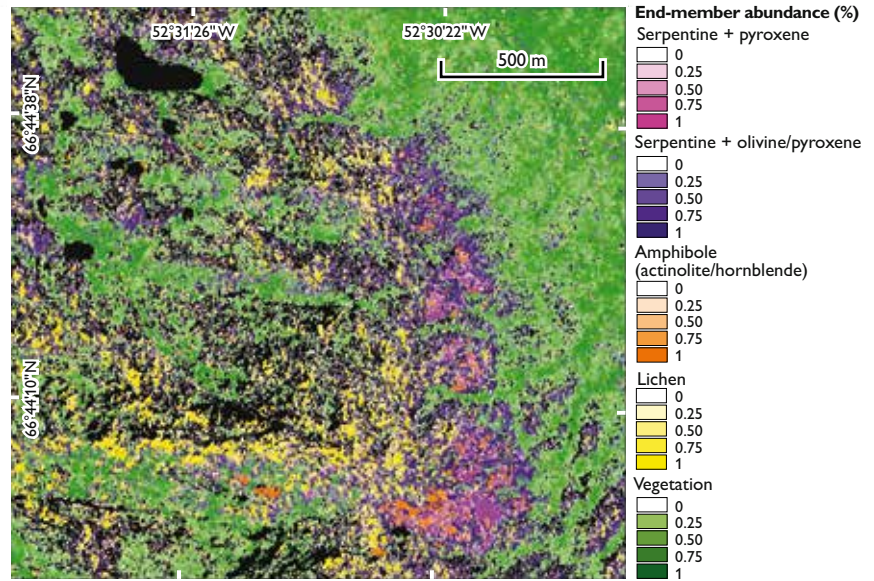

Fig. 2. Spectra of extracted end members compared with selected minerals from the USGS spectral library in ENVI software. **A**: full spectral range. **B**: shortwave infrared range.

Fig. 3. The result of unmixing analysis and the abundance of mafic-ultramafic minerals using HyMAP data. Masked pixels are indicated by black colour.

End-member abundance (%)

Serpentine + pyroxene
0
0.25
0.50
0.75
1

Serpentine + olivine/pyroxene
0
0.25
0.50
0.75
1

Amphibole (actinolite/hornblende)
0
0.25
0.50
0.75
1

Lichen
0
0.25
0.50
0.75
1

Vegetation
0
0.25
0.50
0.75
1

The proposed methodology has the advantage of not requiring *a priori* knowledge about the exact effects of lichens – or any other substance – on the reflectance of the mixtures. Instead, this information is obtained by an automated trial and error process. Therefore, this technique can also be beneficial for identification of sensitive bands and indices for deconvolution of any other mixed spectra, whether synthetic as in this case, or obtained directly from the samples.

Multiscale hyperspectral analysis of lithologies with abundant lichen cover

Two sets of hyperspectral data acquired by airborne HyMap (350–2500 nm) and light-weight Rikola (500–900 nm) sensors were chosen to investigate the potential of visible near infrared and shortwave infrared spectral range for detailed lithological mapping in the Nagssugtoqidian orogen of West Greenland, where an ultramafic rock unit with abundant lichen cover is exposed. The extent to which geological information derived from airborne data is retained in the Rikola
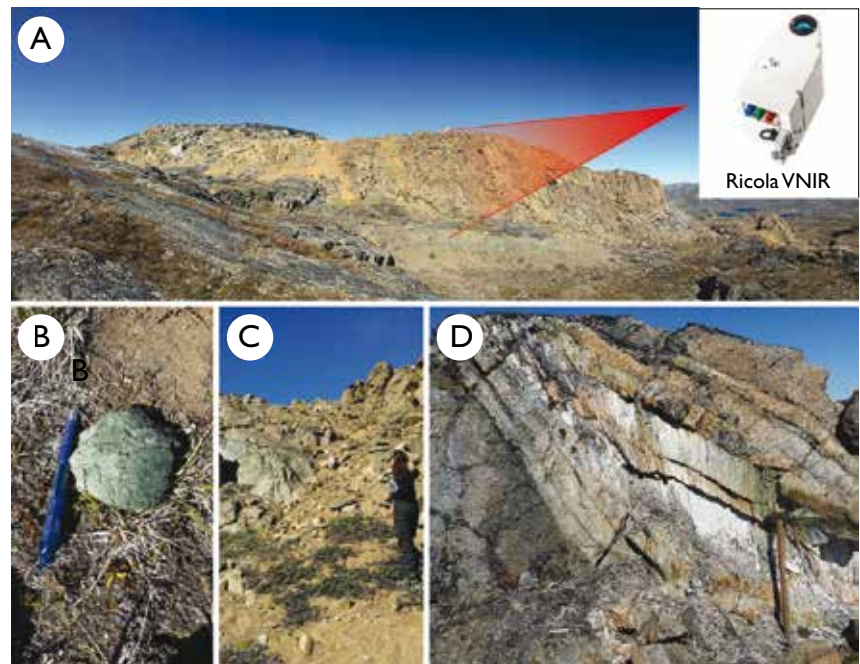

Fig. 4. **A**: Supracrustal rocks in the Innarsuaq region comprising a kilometre-sized body of mafic-ultramafic, looking north. **B**: bright green and black amphibole and biotite at the corner (alteration zone). **C**: Host ultramafic rock; green amphibole to the left and white talc vein in the middle. **D**: 50 cm long asbestos fibres.

53

Legend (C). End-member abundance (%)

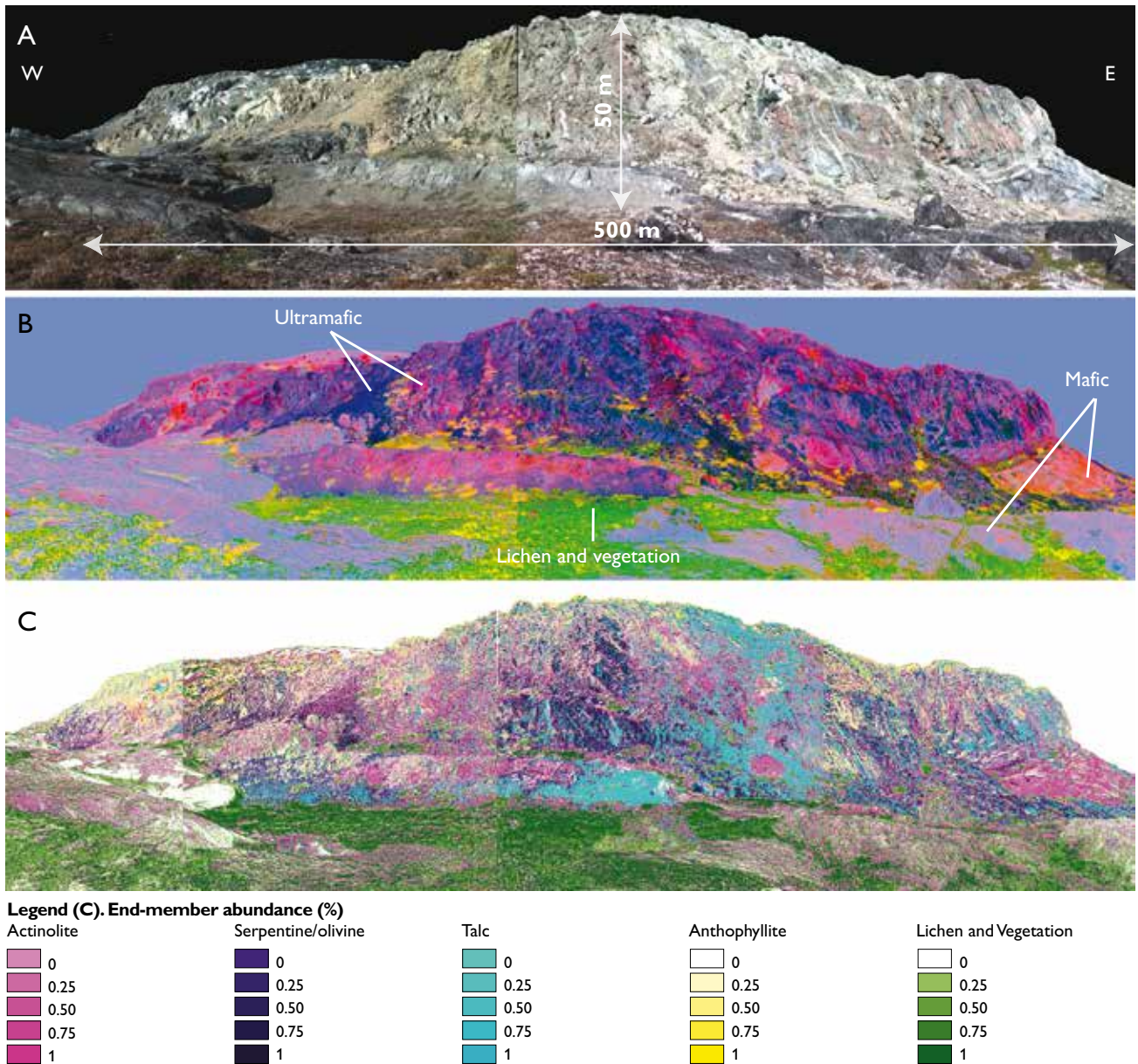| Actinolite	Serpentine/olivine	Talc	Anthophyllite	Lichen and Vegetation
0	0	0	0	0
0.25	0.25	0.25	0.25	0.25
0.50	0.50	0.50	0.50	0.50
0.75	0.75	0.75	0.75	0.75
1	1	1	1	1

Fig. 5. **A**: True-colour hyperspectral image mosaic generated using the Rikola camera. **B**: Minimum Noise Fraction false-colour image: **Red**: Band 6. **Green**: Band 2. **Blue**: Band 1. **C**: result of spectral unmixing analysis and the abundance of mafic-ultramafic minerals.

hyperspectral data, is examined as an insight to future drone-based hyperspectral mapping capabilities and the possibility of extracting valuable mineralogical and lithological information using such platforms.

The airborne hyperspectral dataset is corrected for abnormal pixels and removal of bad bands (such as water vapour absorption features and noisy bands) prior to atmospheric correction. Dark pixels, snow, clouds and water were filtered out. Next, the spatial–spectral end-member extraction method (Rogge *et al.* 2007) is used to derive an image end-member set. This makes an assessment of subtle litho-

logical variability across a given study area possible. These end members are then sorted based on expert knowledge of known spectral features (water, snow, vegetation, lichen and geological materials) followed by a more detailed sorting into individual classes within each category. Subtle shortwave infrared features related to key minerals in the geological materials are particularly important. The resulting sorted end-member classes are subsequently averaged to produce a final end-member set. A final set of six geological end members (Fig. 2), and two end members related to vegetation and lichens are deducted from expert-based analysis. Figure 2

shows a plot of the extracted end members using the spatial–spectral end-member extraction method and the corresponding signatures from the United States Geological Survey (USGS) spectral library (Kokaly *et al.* 2017). The shortwave infrared spectral characteristics of the ultramafic rocks studied here were controlled by amphibole minerals as exemplified by hornblende, actinolite and anthophyllite (Fig. 3). The absorption features in the shortwave infrared region are located at 2320 and 2380 nm and are of the same order of magnitude. The shortwave infrared spectrum of olivine-rich rocks clearly reflects a mixture of antigorite serpentine with a characteristic stronger absorption feature at 2320 nm. A less distinct absorption feature at 2310 nm is present for rocks enriched in talc. Fractional abundances of the end members within the scene are determined using an iterative implementation of spectral mixture analysis method (Rogge *et al.* 2007).

The interpretation of HyMap data revealed a number of mafic and ultramafic complexes in the border area between the parautochthonous and allochthonous zones of the Nagssugtoqidian orogen. One such complex occurs to the east of the head of the fjord Kangerluarsuk, here referred to as Innarsuaq (see fig. 1 of Salehi & Thaarup 2018, this volume). As can be seen from Fig. 3, the predictive map from the Innarsuaq area displays a complex distribution of exposed bedrock, a feature confirmed during a brief field visit. The results were validated using expert knowledge of spectral characteristics of lichens and mineralogy, as well as spectral measurements of field samples and associated XRD results.

The Rikola camera was operated in ground-based mode and panned stepwise to acquire a set of five overlapping images. The images were corrected for geometric, radiometric and topographic effects and stitched to a continuous mosaic (Figs 4, 5). The distribution of lithological units were then mapped using the Minimum Noise Fraction method (Kruse *et al.* 1993).The information regarding mineral abundances were retrieved using the Spectra Unmixing procedure (Fig. 5).

Conclusions

1. Lichen effects on the spectra of their rock substrate have important implications for the geological analysis of airborne/spaceborne hyperspectral data where rock-encrusting lichens partially obscure exposed bedrock.

2. Analysis of airborne hyperspectral data can result in high-quality regional mapping products capable of discriminating geological materials of interest based on subtle spectral differences. The map product generated from the Rikola scenes in this study captures the broad geological patterns and many of the lithologies generated from the airborne data, although some spectral and lithological discrimination is lost due to its more limited wavelength range.

3. The performance of hyperspectral data acquired from different platforms and at various scales is investigated for qualitative mapping of arctic mineral resources in the presence of abundant lichens. The application of such technologies to extract detailed geological information from complex inaccessible regions of Greenland certainly has a very low cost/benefit ratio in comparison to traditional geological fieldwork. Future space-borne hyperspectral sensors will offer new possibilities to expand the scale of mapping in Greenland. Integration with other remote sensing datasets such as magnetic data will simplify mineral exploration and geological mapping in the Arctic.

Acknowledgments

References

Clark, R.N. & Roush, T.L. 1984: Reflectance spectroscopy: Quantitative analysis techniques for remote sensing applications. Journal of Geophysical Research: Solid Earth **89**(B7), 6329–6340.

Kokaly, R.F., Clark, R.N., Swayze, G.A., Livo, K.E., Hoefen, T.M., Pearson, N.C., Wise, R.A., Benzel, W.M., Lowers, H.A., Driscoll, R.L.& Klein, A.J. 2017: USGS Spectral Library Version **7**. U.S. Geological Survey Data Series **1035**, 61 pp., *http://dx.doi.org/10.3133/ds1035*

Kruse, F.A., Lefkoff, A., Boardman, J., Heidebrecht, K., Shapiro, A., Barloon, P. & Goetz, A. 1993: The spectral image processing system (SIPS) – interactive visualization and analysis of imaging spectrometer data. Remote Sensing of Environment **44**, 145–163

Rogge, D.M., Rivard, B., Zhang, J., Sanchez, A., Harris, J., & Feng, J. 2007: Integration of spatial–spectral information for the improved extraction of endmembers. Remote Sensing of Environment **110**, 287–303.

Salehi, S. & Thaarup, S. 2018: Mineral mapping by hyperspectral remote sensing in West Greenland using airborne, ship-based and terrestrial platforms. Geological Survey of Denmark and Greenland Bulletin **41**, 47–50 (this volume).

Salehi, S., Karami, M. & Fensholt, R. 2016: Identification of a robust lichen index for the deconvolution of lichen and rock mixtures using pattern search algorithm (case study: Greenland). International Archives of the Photogrammetry, Remote Sensing & Spatial Information Sciences **XLI-B7**, 973–979.

Salehi, S., Rogge, D., Rivard, B., Heincke, B.H. & Fensholt, R. 2017: Modeling and assessment of wavelength displacements of characteristic absorption features of common rock forming minerals encrusted by lichens. Remote Sensing of Environment **199**, 78–92.

Author's address

S.S., *Geological Survey of Denmark and Greenland, Øster Voldgade 10, DK-1350 Copenhagen K, Denmark.* E-mail: *ssal@geus.dk*.